DOI:
10.1016/j.jinorgbio.2017.12.007

Document Version
Peer reviewed version

Accepted Manuscript

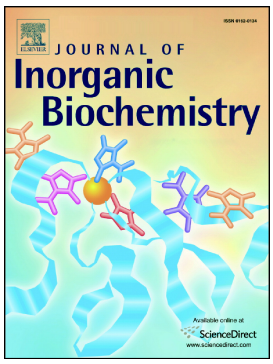

The interaction of pyridoxal isonicotinoyl hydrazone (PIH) and salicylaldehyde isonicotinoyl hydrazone (SIH) with iron

Yu-Lin Chen, Xiaole Kong, Yuanyuan Xie, Robert C. Hider

PII: S0162-0134(17)30679-7
DOI: https://doi.org/10.1016/j.jinorgbio.2017.12.007
Reference: JIB 10394

To appear in: *Journal of Inorganic Biochemistry*

Received date: 28 September 2017
Revised date: 6 December 2017
Accepted date: 10 December 2017

Please cite this article as: Yu-Lin Chen, Xiaole Kong, Yuanyuan Xie, Robert C. Hider , The interaction of pyridoxal isonicotinoyl hydrazone (PIH) and salicylaldehyde isonicotinoyl hydrazone (SIH) with iron. The address for the corresponding author was captured as affiliation for all authors. Please check if appropriate. Jib(2017), https://doi.org/10.1016/j.jinorgbio.2017.12.007

The Interaction of Pyridoxal Isonicotinoyl Hydrazone (PIH) and Salicylaldehyde Isonicotinoyl Hydrazone (SIH) with Iron.

Yu-Lin Chen[1], Xiaole Kong[1], Yuanyuan Xie[2] and Robert. C. Hider[1]*

ABSTRACT

The interaction of pyridoxal isonicotinoyl hydrazone (PIH) and salicylaldehyde isonicotinoyl hydrazone (SIH), two important biologically active chelators, with iron has been investigated by spectrophotometric methods. High iron(III) affinity constants were determined for PIH, $\log\beta_2$=37.0 and SIH, $\log\beta_2$=37.6. The associated redox potentials of the iron complexes were determined using cyclic voltammetry at pH7.4 as +130mV (*vs* normal hydrogen electrode, NHE) for PIH and +136mV(*vs* NHE) for SIH. These redox potentials are much higher than those corresponding to iron chelators in clinical use, namely deferiprone, -620mv; desferasirox, -600mv and desferrioxamine, -468mv. Although the positive redox potentials of SIH and PIH are similar to that of EDTA, namely +120mV, the iron complexes of these two hydrazone chelators, unlike the iron complex of EDTA, do not redox cycle in the presence of vitamin C. These properties render PIH and SIH as excellent scavengers of iron, under biological conditions. Both SIH and PIH scavenge mononuclear iron(II) and iron(III) rapidly. These fast kinetic properties of the hydrazone-based chelators provide a ready explanation for the adoption of SIH in fluorescence-based methods for the quantification of cytosolic iron(II).

1. Institute of Pharmaceutical Sciences, King's College London. 150 Stamford Street London SE1 9NH UK
2. Key Laboratory for Green Pharmaceutical Technologies and Related Equipment of Ministry of Education, Zhejiang University of Technology, P.R. China.

*Email: robert.hider@kcl.ac.uk; Tel: +442078484882. Fax:+442078486394

1. Introduction

Pyridoxal isonicotinoyl hydrazone (PIH, **1**) was initially identified as an iron chelator which possesses interesting biological properties in 1979 by Ponka and coworkers [1,2]. Subsequent studies demonstrated that PIH was effective at scavenging and excreting iron from a range of *in vitro* and *in vivo* models [3-8]. PIH is a tridentate ligand (**1**) coordinating iron(III) *via* two oxygen atoms and one nitrogen [9]. Its ability to scavenge iron from iron-overloaded tissues is related to its relatively low molecular weight, logP value and uncharged nature [10], all of which facilitate the entry of PIH into cells. In addition, the 2:1 iron complex possesses a favourable logP value and a low charge density and so is able to efflux from cells by non-facilitated diffusion". Preliminary studies in animals and man have demonstrated relatively low toxicity [12].

PIH and many of its analogues possess anti-proliferative activity [13,14,15] and consequently have potential in the treatment of cancer [16]. Furthermore, this hydrazone family of chelators possess strong antioxidant properties [17,18]. By virtue of their ability to rapidly enter cells, PIH and salicylaldehyde isonicotinoyl hydrazone (SIH) have also been extensively adopted by cell biologists to perturb intracellular iron levels [19-21]. Indeed SIH has found wide application in the calcein-based assay for monitoring the cytosolic labile iron pool [22-24]. Despite this wide use, there have been few reports of iron affinity constant measurements relating to PIH, two with iron(III) [25,26] and one with iron(II) [27]. The reported pFe^{3+} value of 22.9 [26] (as corrected for $[L]_{Total}=10^{-5}M$) is similar to that of the tridentate chelators deferasirox (22.5)[28] and deferitazole (22.3) [29]. As with PIH, there are few reports of iron(III) affinity constants for SIH [30]. Indeed there is some uncertainty regarding the potentiometrically determined affinity constants of both PIH and SIH [30]. In view of the central importance of these two molecules, we decided to investigate their interaction with both iron(III) and iron(II).

2. Experimental section

^{1}H NMR and ^{13}C NMR spectra were measured on a Varian 400(400MHz) spectrometer (chemical shifts in δ ppm) using TMS as internal standard. Mass spectra (ESI-MS) were determined on a Thermo Finigan LCQ-Advantage. IR Spectra were determined on a Nicolet Avatar-370 spectrometer in KBr (ν in cm^{-1}). Melting points were measured on a Büchi B-540 capillary melting point apparatus.

2.1 Materials

PIH was purchased from Santa Cruz Biotechnology, Heidelberg, Germany. Iron salts, glutathione and deferiprone were purchased from Sigma (www.sigmaaldrich.com)

2.2 Preparation of SIH

This synthesis utilised the method reported by Hassan *et al.*[19] Isoniazide (4.11g, 30mmol) was dissolved in 150mL ethanol at 60°C, then salicylaldehyde (4.03g, 33mmol) was added and the reaction mixture was refluxed for 4h. The solution was cooled to 0°C and a yellow precipitate was obtained by filtration. The crude product was recrystallized from ethanol to give SIH (6.0g, yield 83%) as pale yellow crystals.

N'-(2-Hydroxybenzylidene)isonicotinohydrazide (SIH): Pale yellow solid; m.p. 247.8-248.7°C; IR (KBr): ν_{max} = 3438, 3203, 3006, 1684, 1614, 1568, 1291, 772 cm^{-1}; ^{1}H NMR (400 MHz, DMSO-d_6) δ(ppm): 12.28 (s, 1H, NH), 11.06 (s, 1H, OH), 8.79 (d, 2H, *J* = 6.0Hz, pyridine-H), 8.67 (s, 1H, N=CH), 7.84 (dd, 2H, *J* = 2.0, 4.8 Hz, pyridine-H), 7.60 (dd, 1H, *J* = 1.6, 7.6 Hz, Ar-H), 7.33-7.29 (m, 1H, Ar-H), 6.95-6.90 (m, 2H, Ar-H); ^{13}C NMR (100 MHz, DMSO-d_6) δ(ppm): 160.9, 157.1, 149.9, 148.9, 139.6, 131.3, 129.1, 121.2, 119.1, 118.3, 116.2; MS (ESI): m/z (%) = 240; $C_{13}H_{11}N_3O_2$, requires C, 64.72%; H, 4.60% and N, 17.41%; found, C, 64.72%; H, 4.52% and N, 17.47%.

2.3 pKa and iron stability constants

The automated titration system used in this study comprised of an autoburette (Metrohm Dosimat 765 liter ml syringe) and Mettler Toledo MP230 pH meter with Metrohm pH electrode (6.0133.100) and a reference electrode (6.0733.100). 0.1 M KCl electrolyte solution was used to maintain the ionic strength. The temperature of the test solutions was maintained in a thermostatic jacketed titration vessel at 25°C ± 0.1°C by using a Techne TE-8J temperature controller. The solution under investigation was stirred vigorously throughout titrations. A Gilson Mini-plus#3 pump with speed capability (20 ml/min) was used to circulate the test solution through a Hellem quartz flow cuvette. For the stability constant determinations, a 50 mm path length cuvette was used, and for pKa determinations, a cuvette path length of 10 mm was used. The flow cuvette was mounted on an HP 8453 UV-visible spectrophotometer. All instruments were interfaced to a computer and controlled by a Visual Basic program. Automatic titration and spectral scans adopted the following strategy: the pH of a solution was increased by 0.1 pH unit by the addition of KOH from the autoburette; when pH readings varied by <0.001 pH unit over a 30 s period, they were judged to be stable and the spectrum of the solution was recorded. The cycle was repeated automatically until the defined end point pH value was achieved. All the titration data were analyzed with the pHab program [32]. Species plots were calculated using the HYSS program [33]. The values of $\log K_1$ and $\log\beta_2$, as defined in equations (i) – (iii), were determined by use of the HYSS program [33]. Analytical grade reagent materials were used in the preparation of all solutions.

Equations (i) – (iii) here

In addition to $\log K_1$ and $\log\beta_2$ values, pFe^{3+} values have been adopted by chelation chemists as a convenient means of comparing the iron(III) chelating capability of different ligands at pH 7.4. At this pH, there can be appreciable competition for the ligand by protons. In contrast, the $\log K_1$ and $\log\beta_2$

values are based on the values for the equilibrium constant in the absence of proton competition (equations (i) and (ii)).

pFe^{3+} values are determined from logβ values, pKa values, pH and total concentrations of Fe^{III} and ligand. Typically, when comparing iron(III) chelators of clinical interest, the following conditions are adopted; $[Fe^{3+}]_{Total} = 10^{-6}M$; $[Ligand]_{Total} = 10^{-5}M$ and pH = 7.4 [34].

2.4 Electrochemical Measurements

Cyclic voltammetry (CV) measurements were performed with an CS-120 device (Corrtest). Solutions of SIH or PIH (2mM) with iron(III) (1mM) at pH 7.42 (0.1M 3-morpholinopropane-1-sulfonic acid, MOPS, 20% DMSO V/V) were investigated. All measurements were conducted under N_2 in a jacketed, one-compartment cell with a platinum disk working electrode (geometric area: 0.07 cm^2) (Corrtest), a platinum wire counter electrode (Corrtest) and a Ag/AgCl reference electrode. The working electrode surface was polished, sonicated in water, and air-dried immediately before use. The sweep rate was 100 mV/s. O_2 was removed from the electrolyte solution by bubbling N_2 through the solvent for several minutes prior to measurement. A N_2 atmosphere was continuously maintained above the solution while the experiments were in progress. The temperature was controlled by using a double-jacketed cell and a thermostat with water bath at 25 ºC.

2.5 Kinetic spectrophotometric measurements

All kinetic studies were undertaken at pH 7.4 (25mM MOPS) and 25ºC. The iron concentration adopted throughout was 10μM and the corresponding ligand concentration was chosen based on its dentate number, 30μM for deferiprone, 20μM for SIH and PIH. Iron(II) sulphate was used as a source of iron(II) and the solutions were prepared immediately before use. Iron(III) nitrate was used as a source of iron(III), again the solutions being prepared immediately before use. The usual practice of using iron(III)

nitrilotriacetic acid (NTA) solutions was not adopted because NTA interferes with kinetics of iron substitution. The glutathione concentration was 2mM. The UV-Visible spectra were recorded by an HP 8453 UV-visible spectrophotometer with a 50mm Hellem quartz flow cuvette being circulated by a Gilson Mini-plus #3 pump – speed capability (20mL/min), controlled by in-house computer software.

3. Results

3.1 Determination of pKa values

PIH was found to be relatively stable over the pH range 1-10, in contrast to SIH which was found to be unstable at pH values less than 2 (Figure S1 supplementary data). This is likely to result from the hydrolysis of the Schiff base. Thus exposure of this ligand to pH values < 2.0 was avoided during titration studies.

The spectrophotometric analysis of the titrations of PIH and SIH (Figure 1) were fitted to four and three pKa values respectively. The corresponding pKa values are given in Table 1. There is good agreement with the study of Richardson *et al* [35] and although we agree with their assignment of pKa values for SIH, as indicated in figure 2, we do not agree with the previous assignment of values for PIH. Based on studies by Metzler and Snell [36], Richardson assigned their measured pKa value of 4.20 to the phenolic function [35]. However, titration of 3-hydroxypyridine and its analogue, pyridoxine, follows the sequence indicated in equation (iv) [37,38]. Based on these studies, we propose the pKa assignments for PIH are as indicated in figure 2. These assignments are close to those calculated for PIH by Marvin [39]. The influence of pH on the speciation plots of the two ligands is presented in figure 3. With both compounds, there is a mixture of the non-charged species and the monoanionic species at pH 7.4.

Equation (iv) here.

3.2 Determination of the iron(III) affinity constants

PIH and iron(III) were titrated in a 2:1 molar ratio against KOH over the pH range 1.3-7.5. There is an isosbestic point at 475 nm with the λ max shifting from 473 to 465 nm (Figure S2, supplementary data). The data is consistent with the formation of two complexes, namely Fe·(PIH) and Fe·$(PIH)_2$. The affinity constants $logK_1$ and $log\beta_2$ were determined as 20.3 and 37.0. (Table 1). The speciation plot of the iron(III)-PIH system is presented in figure 4A, where the dominant complex at pH 7.4 is $[Fe^{III}(PIH)_2]^-$. The $log\beta_2$ value of 37.0 is larger than the value reported by Vitolo *et al* [26], namely 30.4. SIH and iron(III) were titrated in a 2:1 molar ratio against KOH over the pH range 2.0-5.0 (Figure S3, supplementary material). There is an isosbestic point at 665 nm and the data is consistent with the formation of two complexes, namely Fe·(SIH) and Fe·$(SIH)_2$. The affinity constants $logK_1$ and $log\beta_2$ were determined as 19.3 and 37.6 which are much lower than those previously reported, namely 38.3 and 56.0 [26]. The speciation plot of the iron(III)-SIH system is presented in figure 4B, where the dominant complex at pH 7.4 is $[Fe^{III}(SIH)_2]^-$.

3.3 Determination of the oxidation potentials of the iron complexes of PIH and SIH

Due to the limited solubility of the complexes, cyclic voltammetry was performed at pH 7.45 in the presence of 20% DMSO (by volume) with a molar ratio of ligand: iron of 2:1. The solutions were buffered with MOPS (0.1M). The voltammograms for PIH/iron behave in a semi-reversible manner (Figure 5). The measured electrode potential is +130mV (vs NHE). A similar electrode potential was obtained for SIH, namely +136mV (vs NHE). The stability constants for iron(II) were calculated from the corresponding iron(III) stability constants and the electrode potential, using a standard thermodynamic cycle as $E_{complex}(Fe^{3+}/Fe^{2+}) = E(Fe^{3+}/Fe^{2+}) - 59.15*(log\beta Fe^{3+} - log\beta Fe^{2+})$. Values of $log\beta_2(Fe^{2+})$ for PIH and SIH were determined as 26.1 and 26.9 respectively. These values are higher the

those previously reported for PIH, namely 12.47 [26].

3.4 Kinetic studies of vitamin C oxidation

As the redox potential of ascorbate, under physiological conditions, is in the region of +100mV [40], PIH and SIH iron complexes are predicted to redox cycle in a similar fashion to that of the iron complexes of NTA and EDTA. However, whereas the iron(III) complexes of both these aminocarboxylate ligands readily oxidise reduced vitamin C (300μM at pH 7.4) as monitored at 265nm, the iron(III) complexes of SIH and PIH do not oxidise vitamin C, behaving like the iron(III) complexes of deferiprone and desferrioxamine (Data not presented). In order to confirm this behaviour we coupled vitamin C with dichlorophenolindophenol where the coupled dye enabled measurement of the redox process at 700nm, (equation (v)) [41]. Again, we found that whereas the iron(III) complexes of deferiprone, desferrioxamine, SIH and PIH do not oxidise reduced vitamin C, the iron(III) complexes of NTA and EDTA do (Figure 6).

Equation(v) here

Thus although the redox potentials of the iron complexes of both SIH and PIH are similar to those of NTA and EDTA, they are kinetically much slower. This difference almost certainly results from the effective steric blocking by the two chelating ligands, effectively preventing access to the coordinated iron(III). In contrast, with the aminocarboxylate iron(III) complexes, there is a vacant coordinative site in both iron(III) complexes [42], which are readily accessible to the approach by other ligands and reactants.

3.5 Kinetic studies of iron complex formation

The visible spectra of iron(III)$(SIH)_2$, iron(II)$(SIH)_2$, iron(III)$(PIH)_2$ and iron(II)$(PIH)_2$ at pH 7.4 are presented in figure 7. With both ligands, the spectra of the iron(II) complexes extends to higher wavelengths, with a shoulder for iron(II)$(SIH)_2$ at 550nm and a shoulder for iron(II)$(PIH)_2$ at 490nm (Figure 7). PIH and SIH scavenge both iron(II) and iron(III) rapidly at pH 7.4 with no apparent redox

reaction. Thus both ligands chelate iron(II) (presented as $FeSO_4$) rapidly (complete within 3 min), forming the respective iron(II) complexes and with iron(III) (presented as iron(III)$(NO_3)_3$), although this latter process takes slightly longer to complete, approximately 10 min. (Data not presented). These findings confirm that PIH and SIH bind both iron(II) and iron(III) with relatively high affinity.

The behaviour of both PIH and SIH contrasts markedly with that of deferiprone (**3**), a 3-hydroxypyridin-4-one. When deferiprone is incubated with iron(II) at pH 7.4 the iron(III) (deferiprone) complex is formed extremely rapidly (< 1min) [43,44] (Figure 8A). Thus as with deferrioxamine, rapid autoxidation occurs [45] due to the affinity of deferiprone for iron(II) being much lower than for iron(III) [43]. Surprisingly however deferiprone scavenges iron(III), when presented as the nitrate salt, much more slowly than both SIH and PIH (Figure 8B). Complete chelation of iron(III) at pH 7.4 takes approximately 30 min. We interpret this difference as resulting from the relatively slow rate of exchange of Fe^{III}-OH bonds when compared to Fe^{II}-OH bonds [46]. This renders the rate of substitution of OH^- functions by a ligand much slower for iron(III) than iron(II) (equation vi). The position of equilibrium for this reaction will be strongly influenced by the value of the K_1 affinity constant of the ligands under consideration. The $\log K_1$ values for SIH and PIH are of the order of 20 (Table 1), whereas the corresponding value for deferiprone is 14 [47]. This offers a clear explanation for differences in the rate of scavenging iron(III) at pH 7.4.

Equation (vi) here

A knowledge of the rates at which SIH and deferiprone scavenge different forms of iron is important for the interpretation of the mode of action of fluorescent probes, when the quenching of the latter is used to quantify cytosolic iron(II) levels [48]. As iron(II) glutathione is the major species of labile iron in both the cytosol and the lumen of the mitochondrion [49.50], it was decided to repeat the above chelation studies with

iron(II) in the presence of glutathione (2mM). Again, PIH and SIH were able to scavenge iron from Fe^{II}-GS, rapidly (complete with 3 min), the redox state of the scavenger iron was iron(III) (Fig 9A). We interpret this redox reaction as resulting from the formation of mixed glutathione/SIH complexes equation (vii). With deferiprone, iron scavenging is much slower in the presence of glutathione (2mM) (Fig 9B) and again this reflects the differences in the $\log K_1$ values for iron(III).

4. Discussion

4.1 Affinity constants for iron(III) and iron(II)

As outlined in the introduction, both the hydrazone chelators PIH and SIH have been extensively adopted by cell biologists and biomedical scientists because of their high binding affinity for iron. Despite this wide use, there is some uncertainty regarding the published affinity constants for both iron(II) and iron(III). With the two chelators, depending on the pH, both the 1:1 and 2:1 iron(III) complexes can be characterised. The iron(III) $\log\beta_2$ value determined for PIH in this work, namely 37.0, is somewhat higher than that previously reported [25,26]. Furthermore, favoring the assignment of the pKa value 4.4 to the ring N of the pyridoxine moiety, influences the calculation for the determination of pFe^{3+} values. The value resulting from this work ($[Fe^{3+}]_{total}=10^{-6}$M, $[PIH]_{total}=10^{-5}$M, pH7.4）is 26.2, which is lower than the previously published value of 27.7 [26]. However, the previous workers adopted different conditions for pFe^{3+}, namely $[Fe^{3+}]_{total}=10^{-6}$M, $[PIH]_{total}=10^{-3}$M, pH7.4. Applying these conditions to the data determined in this work leads to the higher value of 30.4. As indicated in the Experimental Section, the generally accepted conditions for pFe^{3+} calculations, as applied to clinically useful iron chelators are $[Fe^{3+}]_{total}=10^{-6}$M and $[Ligand]_{total}=10^{-5}$M, pH 7.4 [34]. We therefore suggest the pFe^{3+} value of 26.2 being adopted for PIH. (Table 1)

The iron(III) $\log\beta_2$ value for SIH, as determined in this work, is similar to that of PIH, namely 37.6,

which corresponds to a pFe^{3+} value of 24.6. These two values would appear to be appropriate for tridentate iron(III) selective chelators (Table 2), the value for PIH falling at the higher end of the range for tridentate ligands. Indeed, these values are greater than the pFe^{3+} values generally assessed to be suitable for scavenging iron in biological matrices (i.e. $pFe^{3+} \geqslant 20$) [51].

We found that the two hydrazone iron complexes possess higher redox potentials than the three iron chelators in current clinical use, namely desferoxamine, -468mV; deferasirox, -600mV; deferiprone, -620mV, respectively [52,53]. This difference in properties is associated with the two hydrazone chelators possessing an appreciable affinity for iron(II) [51] (Table 1). The positive redox potentials of SIH, +136mV, and PIH, +130mV, are similar to that of EDTA, namely +120mV [17]. Therefore, the iron complex of these two hydrazone chelators, like the iron complex of EDTA, might be expected to redox cycle, *via* the Fenton reaction, under physiological conditions [17]. However, this is not the case, as demonstrated in figure 6, where both the hydrazone chelators failed to trigger appreciable vitamin C oxidation. This finding offers a clear explanation for the antioxidant protective effect of PIH in the presence of both FeNTA and FeEDTA [17,18] and probably is a result of the two coordinating ligands providing sufficient steric hindrance to minimise access of reagents to the coordinated iron atom.

4.2 Kinetics of iron(II) and iron(III) complex formation

As discussed by other workers, PIH and SIH scavenge labile iron rapidly [20,21,54] and both the iron(II) and iron(III) complexes are kinetically stable, presumably due to the formation of tight octahedral complexes which are resistant to ligand substitution.

In the presence of physiological levels of glutathione, iron(II) is scavenged by PIH and SIH as iron(III) and in many ways behaves in a similar fashion to deferiprone. This finding has important implications for the quantification of cytosolic labile iron by the use of fluorescence probes, as the relevant iron

affinity constants must be used in the calculations [20,55].

Abbreviations

PIH Pyridoxal isonicotinoyl hydrazone

SIH Salicylaldehyde isonicotinoyl hydrazone

MOPS 3-(N-Morpholino)propanesulfonic acid

NHE Normal hydrogen electrode

NTA Nitrilotriacetic acid

References:

1. P. Ponka, J. Borova, J. Neuwirt and O. Fuchs, FEBS Lett. 97 (1979) 317-321.
2. P. Ponka, J. Borova, J. Neuwirt, O. Fuchs and E. Necas, Biochim. Biophys. Acta 586 (1979) 278-297.
3. M. Cikrt, P. Ponka, E. Necas and J. Neuwirt, Brit. J. Haematol. 45 (1980) 275-283.
4. C. Hershko, S. Avramovici-Grisaru, G. Link, L. Gelfand and S. Sarel, J. Lab. Clin. Med. 98 (1981) 99-108.
5. D. K. Johnson, M. J. Pippard, T. B. Murphy and N. J. Rose, J. Pharmacol. Experimental Therap. 221 (1982) 399-403.
6. P. Ponka, R. W. Grady, A. Wilczynska and H. M. Schulman, Biochim. Biophys. Acta 802 (1984) 477-489.
7. E. Baker, M. L. Vitolo and J. M. Webb, Biochem. Pharmacol. 34 (1985) 3011-3017.
8. E. Baker, D. R. Richardson, S. Gross and P. Ponka, Hepatology 15 (1992) 492-501.
9. T. B. Murphy, N. J. Rose, V. Schomaker and A. Aruffo, Inorganica Chim. Acta 108 (1985) 183-194.
10. J. T. Edward, BioMetals 11 (1998) 203-205.
11. J. L. Buss, E. Arduini, P. Ponka, Biochem. Phamacol. 64 (2002) 1689-1701.
12. D. R. Richardson, P. Ponka, J. Lab. Clin. Med. 131 (1998) 306-315.
13. D. R. Richardson, E. H. Tran, P. Ponka, Blood 86 (1995) 4295-4306.
14. J. Gao, D. R. Richardson, Blood 98 (2001) 842-850.
15. E. Mackova, K. Hruskova, P. Bendova, A. Vavrova, H. Jansova, P. Haskova, P. Kovaridova, K. Vavrova, T. Simunek, Chem. Biol. Interact. 197 (2012) 69-79.
16. D. Richardson, Leukemia and Lymphoma 31 (1998) 47-60.

17. H. M. Schulman, M. Hermes-Lima, E. M. Wang, P. Ponka, Redox Report 1 (1995) 373-378.

18. M. Hermes-Lima, P. Ponka, H. M. Schulman, Biochim. Biophys. Acta 1523 (2000) 154-160.

19. Z. I. Cabantchik, P. Milgram, H. Glickstein and W. Breuer, Anal. Biochem. 233 (1995) 221-227.

20. G. Zanninelli, P. Brissot, R. R. Hider, A. P. Konijn, A. Shanzer and Z. I. Cabantchik, Mol. Pharmacol. 51 (1997) 842-852.

21. H. Glickstein, R. B. El, M.Shvartsman and Z. I. Cabantchik, Blood 106 (2005) 3242-3250.

22. A. M. Konijn, H. Glickstein, B. Vaisman, E. G. Meyron-Holtz, I. N. Slotki and Z. I. Cabantchik, Blood 94 (1999) 2128-2134.

23. M. Shvartsman, E. Fibach and Z. I. Cabantchik, Biochem. J. 429 (2010) 185-193.

24. S. Epsztejn, O. Kakhlon, H. Glikstein, W. Breuer and Z. I. Cabantchik, Anal. Biochem. 248 (1997) 31-40.

25. M. L. Vitolo, B. W. Clare, G. T. Hefter and J. Webb, Birth. Defects 23 (1988) 71-79.

26. M. L. Vitolo, G. T. Hefter, B. W. Clare and J. Webb, Inorg. Chim. Acta 170 (1990) 171-176.

27. S. Avramovici-Grisaru, S. Sarel, G. Link and C. Hershko, J. Med. Chem. 26 (1983) 298-302.

28. H. Nick, P. Acklin, R. Lattmann, P. Buehlmayer, S. Hauffe, J. Schupp and D. Alberti, Curr. Med. Chem. 10 (2003) 1065-1076.

29. R. C. Hider, X. Kong, V. Abbate, R. Harland, K. Conlon and T. Luker, Dalton Trans. 44 (2015) 5197-5204.

30. J. L. Buss and P. Ponka, Biochim. Biophys. Acta 1619 (2003) 177-186.

31. H. A. Hassan, M. Abdel-Aziz, G. El-Din, A. A. Abuo-Rahma and H. H. Farag, Bioorg. Med. Chem. 17 (2009) 1681-1692.

32. P. Gans, A. Sabatini and A. Vacca, *Ann. Chim.*, 1999; **89**, 45-49.

33. L. Alderighi , P. Gans, A. Ienco, D. Peters, A. Sabatini and A. Vacca, Coord. Chem. Rev. 184 (1999) 311-318.

34. K. N. Raymond and C. J. Carrano, Acc. Chem. Res. 12 (1979) 183-190.

35. D. R. Richardson, L. M. Vitolo, G. T. Hefter, P. M. May, B. W. Clare, J. Webb and P. Wilairat, Inorg. Chim. Acta 170 (1990) 165-170.

36. D. E. Metzler and E. E. Snell, J. Amer. Chem. Soc. 77 (1955) 2431-2437.

37. A. Albert and J. N Philips, J. Chem. Soc. (1956) 1294-1304.

38. T. A. D. Santos, D. O. Costa, S. S. RochaPita and F. S. Semaan, Ecletica Quimica 35 (2010) 81-86.

39. Marvin Sketch version 5.3.1 Chem Axo Ltd www.chemaxon.com.

40. M. Merkofer, R. Kissner, R. C. Hider, U. T. Brunk and W. H. Koppenol, Chem. Res. Toxicol. 19 (2006) 1263-1269.

41. D. J. van der Jagt, P. J. Garry and W. C. Hunt. Clin. Chem. 32 (1986) 1004-1006.

42. M. D. Lind, M. J. Hamor, T. A. Hamor and J. L. Hoard. Inorg. Chem. 3 (1964) 34-43.

43. Z. D. Liu and R. C. Hider, Medicinal Research Reviews 22 (2002) 26-64.

44. Z. D. Liu and R. C. Hider, Coord. Chem. Reviews 232 (2002) 151-171.

45. J. F. Goodwin and C. F. Whitten. Nature 205 (1965) 281-283.

46. M. Eigen, Pure Applied Chem. 6 (1963) 105-110.

47. R. C. Hider and A. D. Hall, Prog. Med. Chem. 28 (1991) 41-173.

48. Y. Ma, W. Luo, P. J. Quinn, Z. Liu and R. C. Hider, J. Med. Chem. 47 (2004) 6349-6362.

49. R. C. Hider and X. Kong, Biometals 24 (2011) 1179-1187.

50. R. C. Hider and X. Kong, Dalton Transactions 42 (2013) 3220-3229.

51. Y, Ma, T. Zhou, X. Kong and R. C. Hider, Curr. Med. Chem. 19 (2012) 2816-2827.

52. T. Zhou, Y. Ma, X. Kong and R. C. Hider, Dalton Trans. 41 (2012) 6371-6389.

53. M. Merkofer, R. Kissner, R. C. Hider and W. H. Koppenol, Helv. Chim. Acta 87 (2004) 3021-3024.

54. Y. Ma, V. Abbate and R. C. Hider, Metallomics 7 (2015) 212-222.

55. J. E. Dubois, H. Fakhrayan, J. P. Doucet, J. M. El Hage Chahine, Inorg. Chem. 31 (1992) 853-859.

56. R. C. Hider and X. Kong, Nat. Prod. Rep. 27 (2010) 637-657.

Figure 1. Spectrophotometric titration of A, [PIH]= 40uM. pH 2.049 to 11.064 and B, [SIH]= 51.8uM. pH 2.37 to 11.38.

Figure 2. Assignment of pKa values in PIH (**1**) and SIH (**2**). Structure of deferiprone (**3**).

Figure 3. Speciation plots of the ligands over the pH range 0-12; A, PIH and B, SIH.

Figure 4. **A**, Speciation plot of Fe(III)/PIH under conditions: [PIH], 80uM; [Fe^{3+}], 40uM, and **B**, speciation plot of Fe(III)/SIH under conditions: [SIH], 80uM; [Fe^{3+}], 40uM.

Figure 5. A. Cyclic voltammetry scan of PIH:Fe (2:1), [Fe] = 2mM at pH 7.45 (0.1M, MOPS; 20% v/v DMSO); B. Cyclic voltammetry scan of SIH:Fe (2:1), [Fe] = 2mM at pH 7.45 (0.1M, MOPS; 20% v/v DMSO). The measurements were performed between +450 to -500mV with the sweep rate of 100mV/s for 3 to 5 cycles.

Figure 6. Oxidation of vitamin C as monitored by the oxidation of dichlorophenolindophenol; [Fe^{3+}], 10 μM; ◆EDTA, 10 μM; ×(blue), NTA, 20 μM; ■, deferiprone, 30 μM; ▲, SIH. 20 μM; ×(purple), PIH, 20 μM; ●, DFO, 10 μM.

Figure 7. Spectra of PIH (A) and SIH (B); 400-800 nm [iron], 10 μM; [Ligand] 20 μM, pH 7.4 (MOPS, 20 mM). L, ——; LFe^{2+} ·····; LFe^{3+} – – – –.

Figure 8. Chelation of iron by deferiprone [iron], 10 μM, [deferiprone], 30 μM. Spectra recorded every 2 minutes, A, with iron(II) sulphate; B, with iron(III) nitrate.

Figure 9. Competition between iron(II) glutathione and various ligands. Monitored by spectroscopy (400 – 800 nm). Spectra recorded every two minutes. [Fe^{2+}], 10 μM; [GSH], 2 mM; A, PIH, 20 μM; B, SIH, 20 μM; C, deferiprone, 30 μM.

$$[Fe^{III}(H_2O)_6]^{3+} + L^- \overset{K_1}{\rightleftharpoons} [Fe^{III}L(H_2O)_3]^{2+} + 3H_2O \qquad \text{eq(i)}$$

$$[Fe^{III}L(H_2O)_3]^{2+} + L^- \overset{K_2}{\rightleftharpoons} [Fe^{III}L_2]^{+} + 3H_2O \qquad \text{eq(ii)}$$

$$[Fe^{III}(H_2O)_6]^{3+} + 2L^- \overset{\beta_2}{\rightleftharpoons} [Fe^{III}L_2]^{+} + 6H_2O \qquad \text{eq(iii)}$$

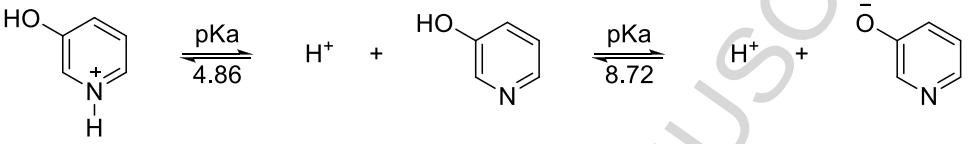

eq(iv)

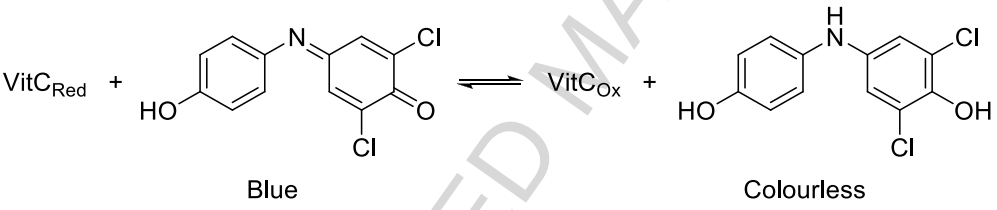

eq (v)

$$Fe^{III}(OH)_6^{3-} + LH + 2H^+ \rightleftharpoons Fe^{III}(OH)_3L^- + 3H_2O \qquad \text{eq (vi)}$$

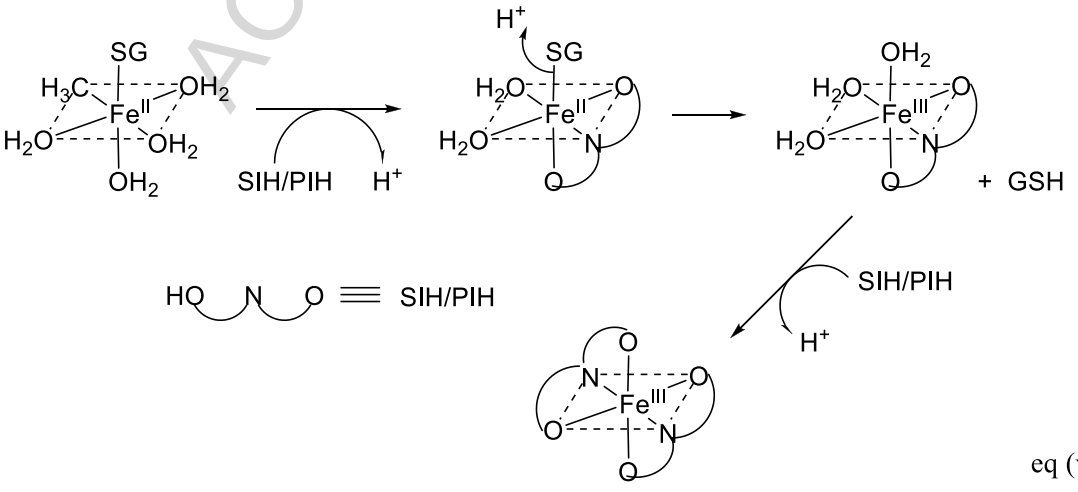

eq (vii)

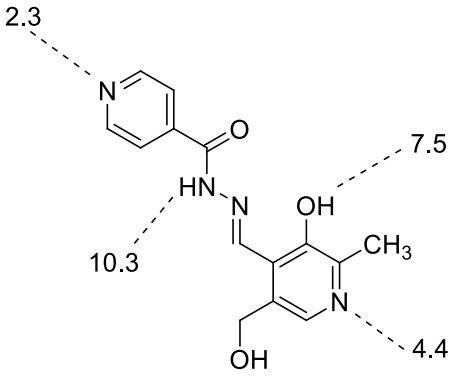

1 (PIH)

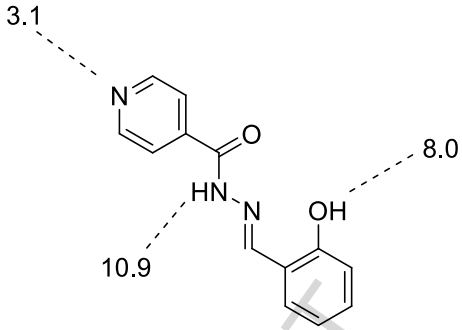

2 (SIH)

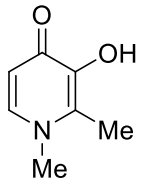

3 (Deferiprone)

Table 1 pKa values and iron(III) affinities and oxidation potentials*.

	pKa	Fe^{3+}	Oxidation potential(NHE)***
SIH	10.9 8.0 3.1	$\log K_1$=19.3 $\log\beta_2$=37.6 pFe^{3+}=24.6**	+136mV
PIH	10.3 7.5 4.5 2.3	$\log K_1$ = 20.3 $\log\beta_2$ = 37.0 pFe^{3+}=26.2**	+130mV

*Repeated experiments can result in about 1% deviation for stability constant values.

**pFe^{3+} under the conditions of $[ligand]_{Total} = 10^{-5}$M, $[Fe^{3+}]_{Total} = 10^{-6}$ M, pH 7.4

***By cyclic voltammetry at pH 7.45 MOPS buffer (0.1M)(20%V/V DMSO).

Table 2 Chelator class and pFe^{3+} values

Chelator	Chelator class	Stoichiometry of dominant complex at pH7	pFe^{3+}
Maltol	Bidentate	3:1	15
N,N-Dimethyl-2,3-dihydroxybenzamide	Bidentate	2:1	15
Deferiprone	Bidentate	3:1	20.4
Deferasirox	Tridentate	2:1	22.5
Deferitazole	Tridentate	2:1	22.3
SIH	Tridentate	2:1	24.6
PIH	Tridentate	2:1	26.2
DFO	Hexadentate	1:1	26.6
MECAM	Hexadentate	1:1	29.1
Enterobactin	Hexadentate	1:1	35.5

pFe^{3+} values taken from references 29 and 56.

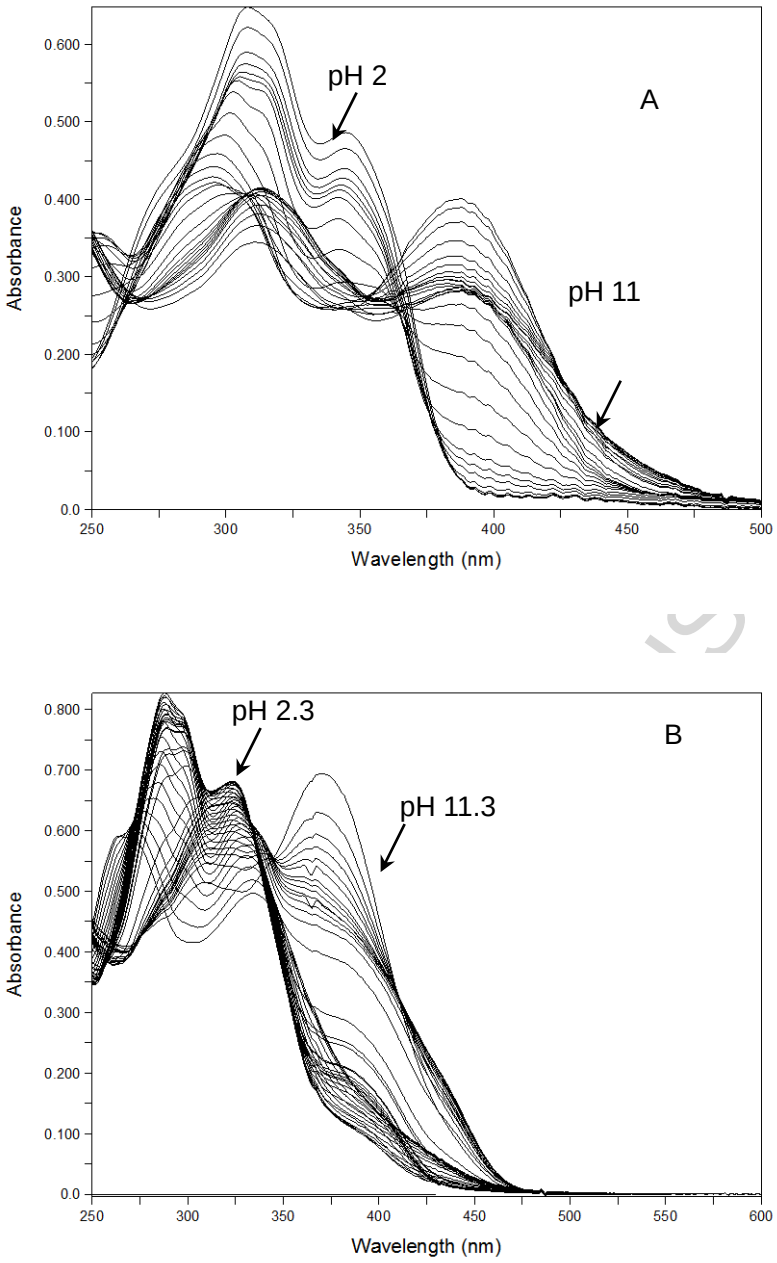

Figure 1

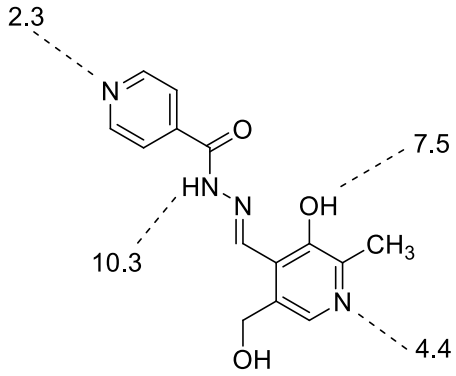

1 (PIH)

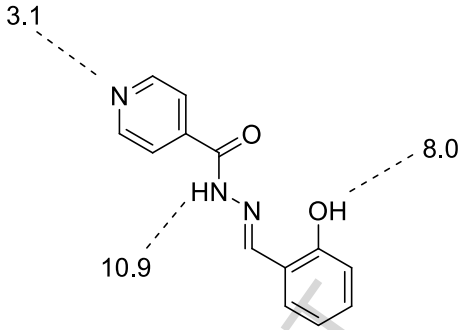

2 (SIH)

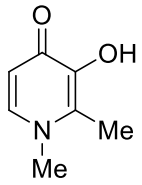

3 (Deferiprone)

Figure 2

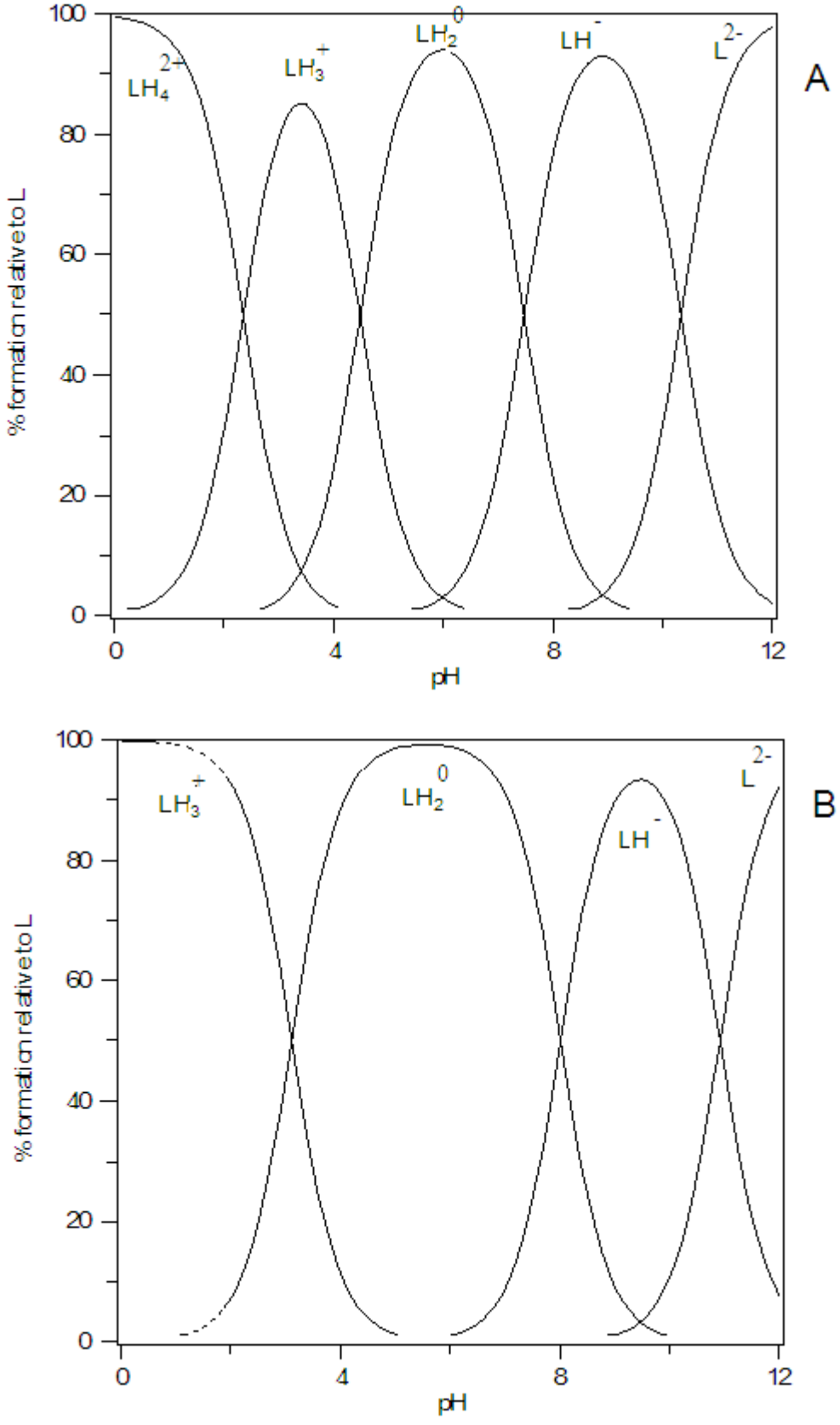

Figure 3

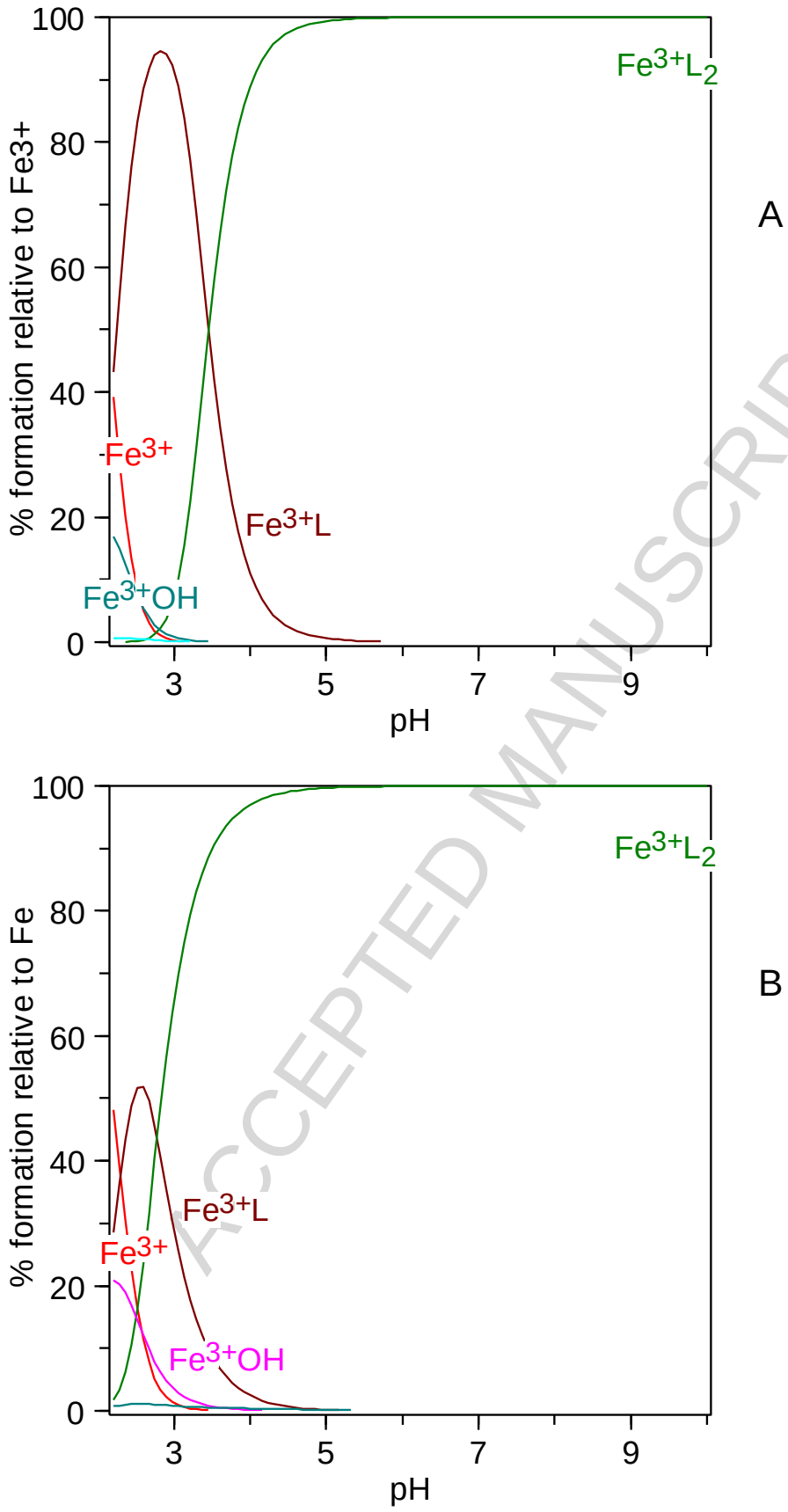

Figure 4

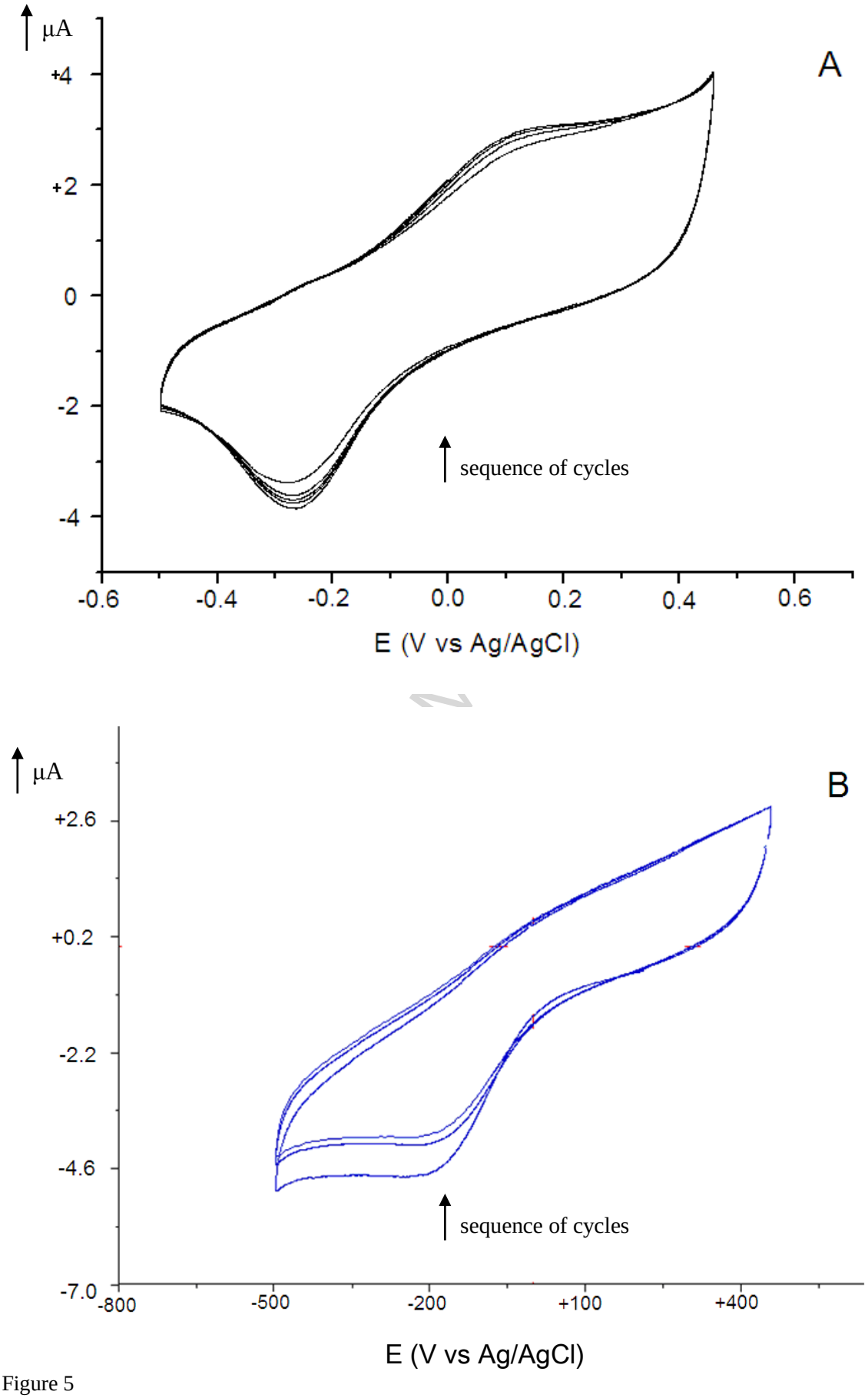

Figure 5

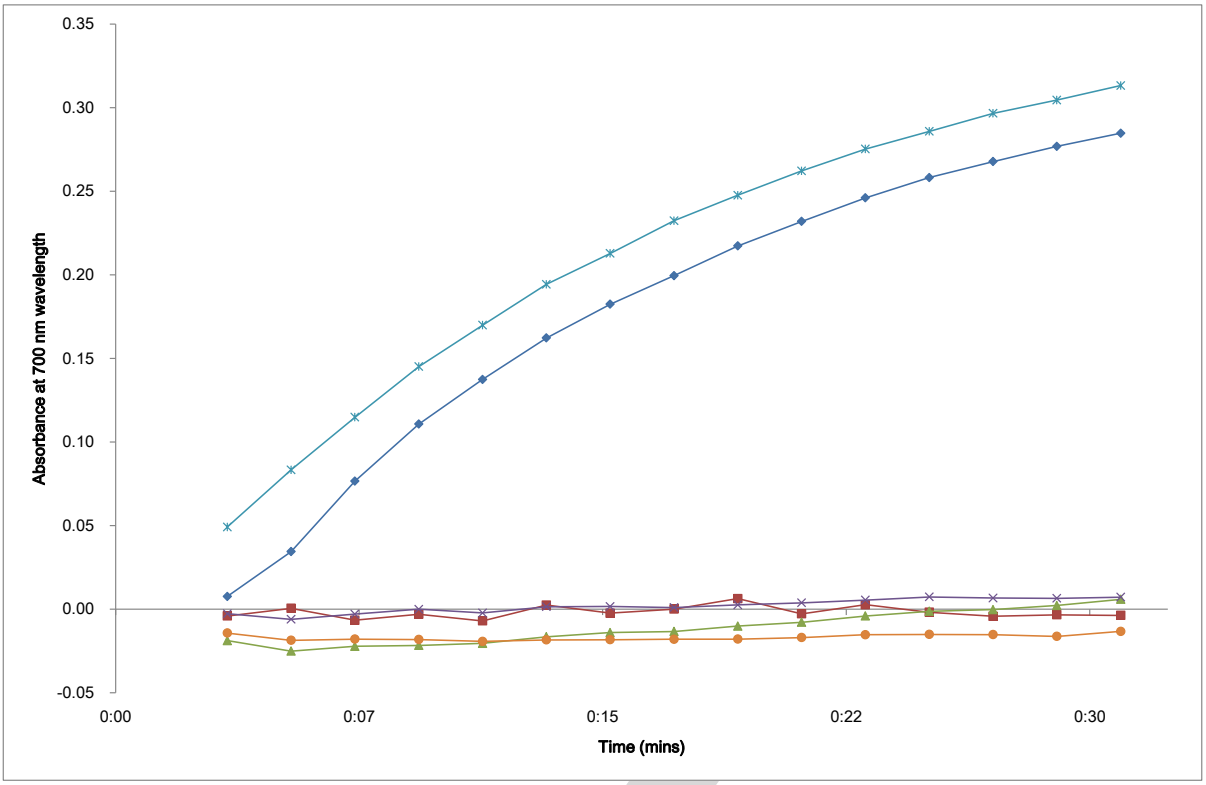

Figure 6

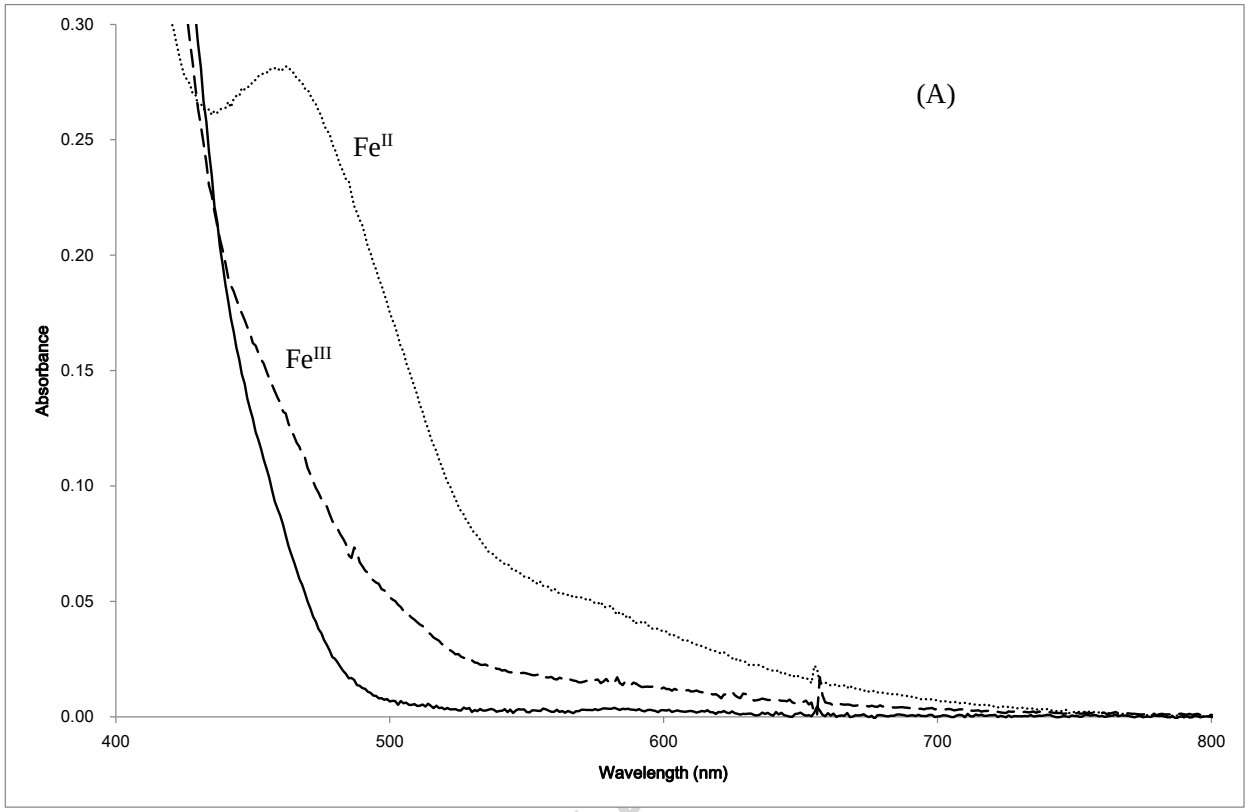

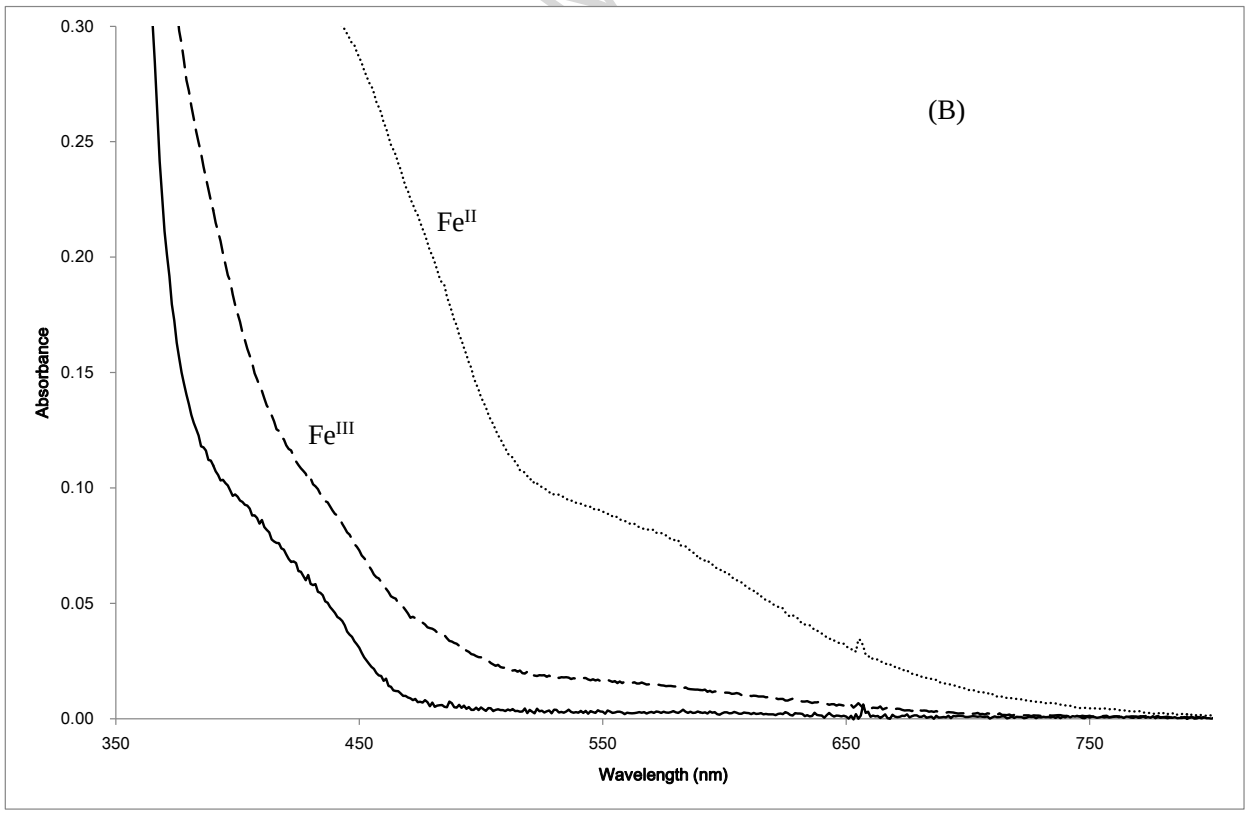

Figure 7

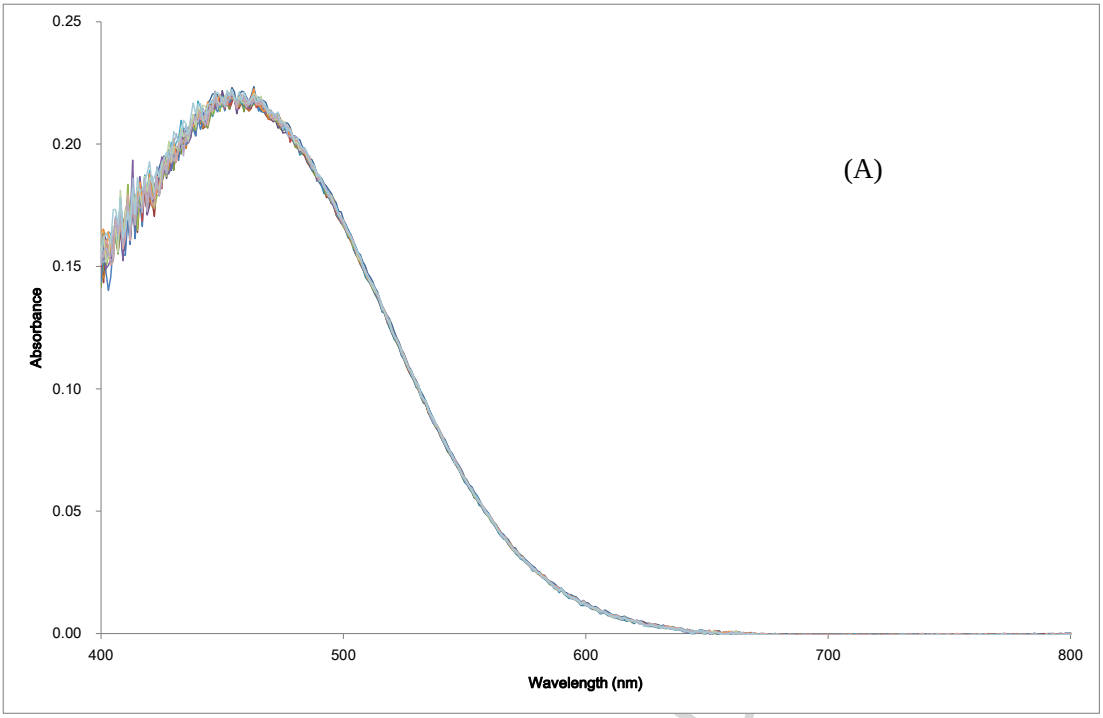

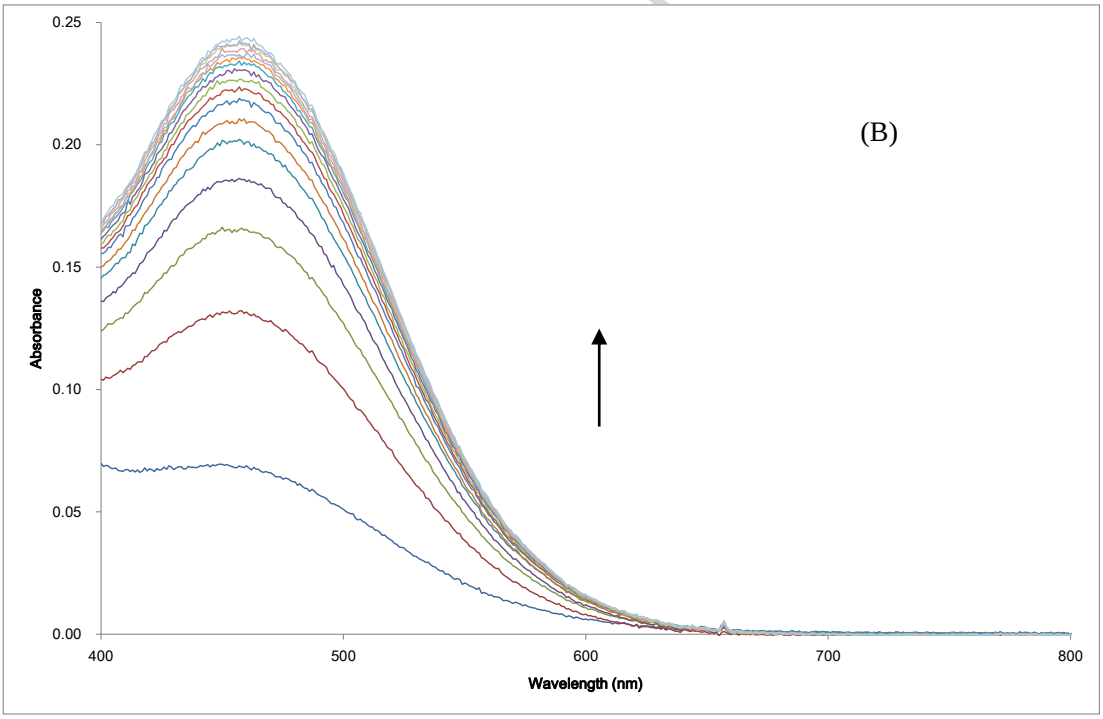

Figure 8

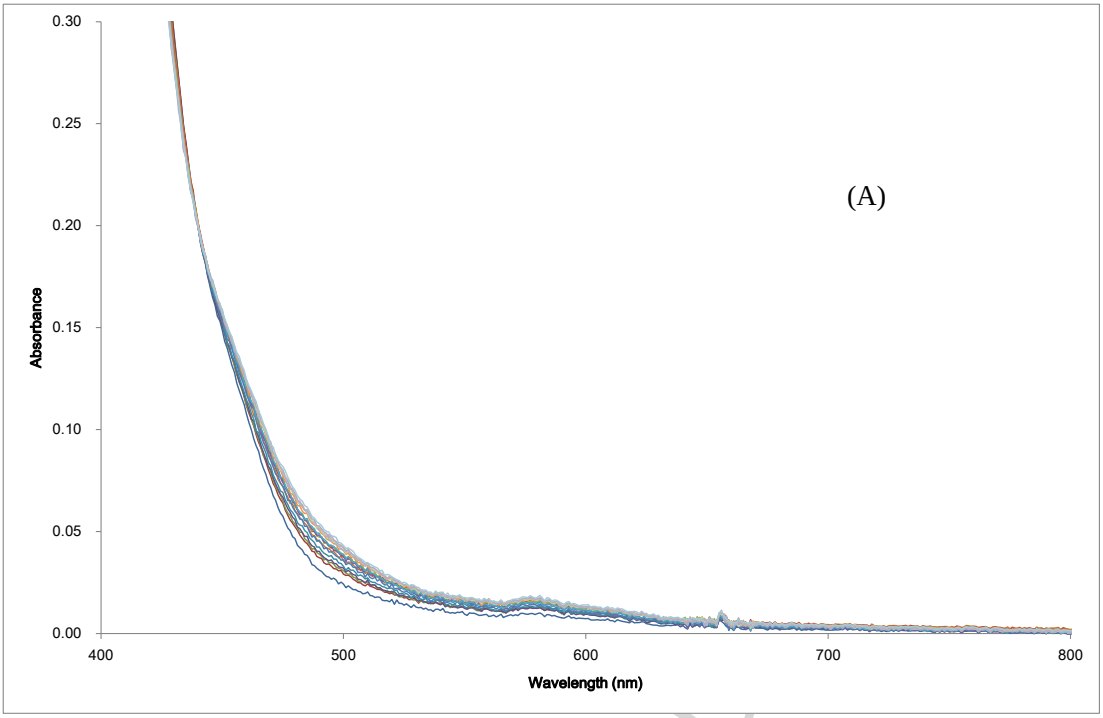

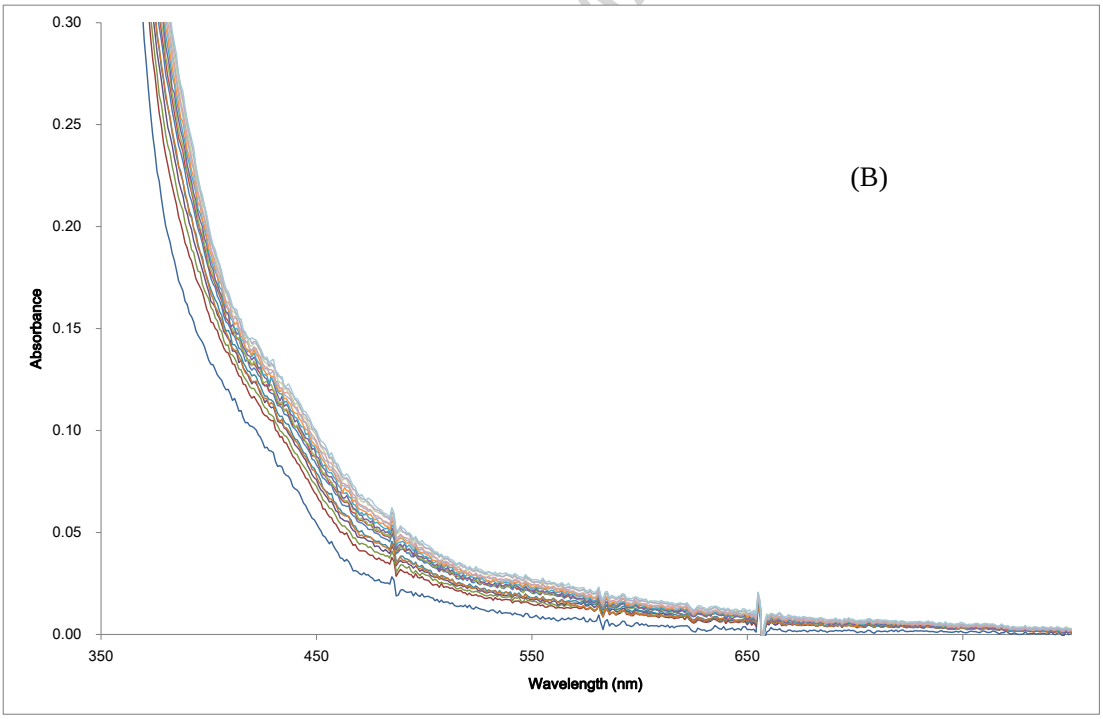

Figure 9 (part)

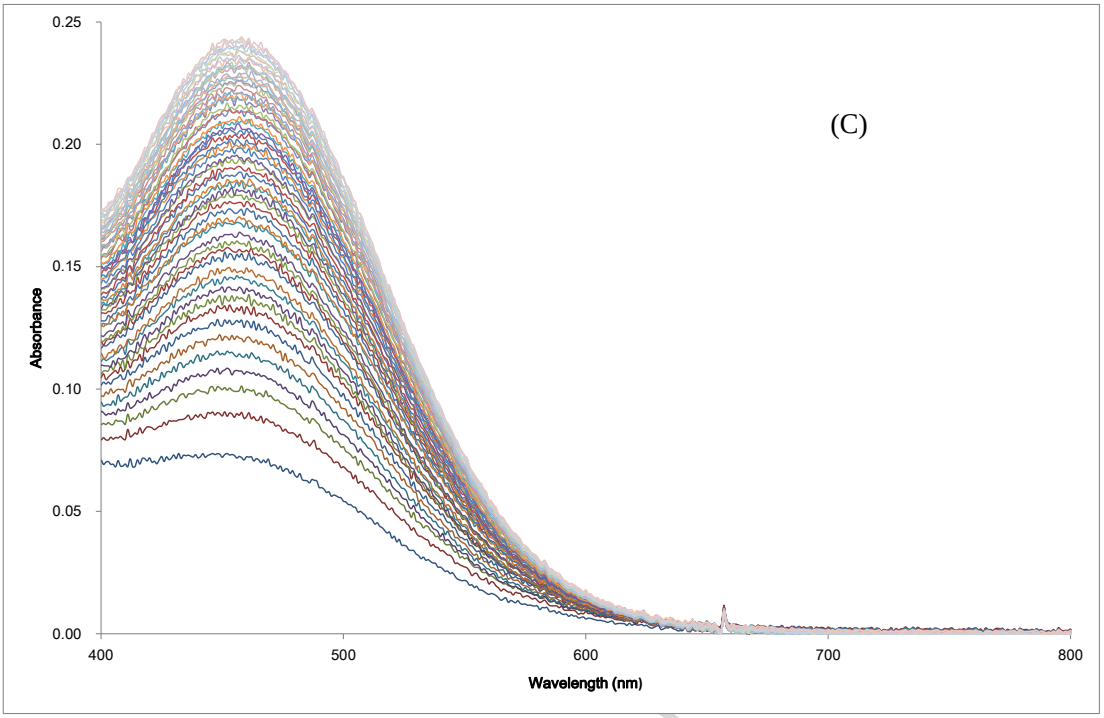

Figure 9 (part)

Graphical abstract

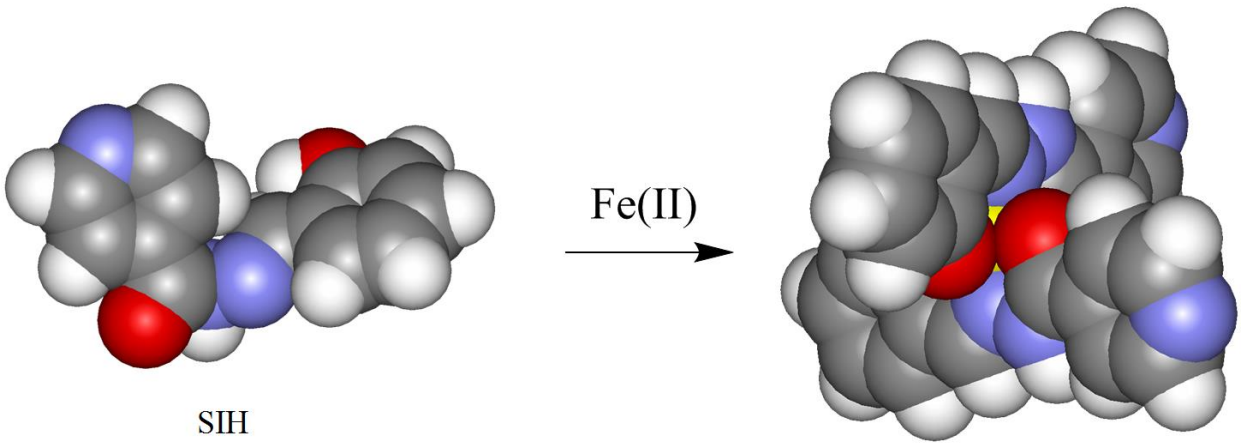

SIH

$Fe^{II}(SIH)_2$

Synopsis

The hydrazone chelators pyridoxal isonicotinoyl hydrazone (PIH) and salicylaldehyde isonicotinoyl hydrazone (SIH) bind both iron(II) and iron(III) with high affinity. The tridentate ligands completely encompass the coordinated iron which renders it inaccessible to other potentially reactive molecules, including oxidising agents, reducing agent and complexing agents.

Highlights

- Updated value for $\log\beta_2(Fe^{3+})$ for pyridoxal isonicotinoyl hydrazone (PIH) is 37.0.
- Updated value for $\log\beta_2(Fe^{3+})$ for salicylaldehyde isonicotinoyl hydrazone (SIH) is 37.6.
- Updated pFe^{3+} values for PIH and SIH are greater than 24.
- The iron complexes of PIH and SIH are not redox active under biological conditions.
- Both PIH and SIH bind iron(II) and iron(III) extremely rapidly.